Microenergy acoustic pulse therapy restores function and structure of pelvic floor muscles after simulated birth injury

Guiting Lin[1], Michelle Van Kuiken[1], Guifang Wang[1], Lia Banie[1], Yan Tan[1], Feng Zhou[1], Zhao Wang[1], Yinwei Chen[1], Yingchun Zhang[2], Tom F. Lue[1]

[1]Knuppe Molecular Urology Laboratory, Department of Urology, School of Medicine, University of California, San Francisco, CA, USA;
[2]Department of Biomedical Engineering, University of Houston, Houston, TX, USA

Contributions: (I) Conception and design: G Lin, Y Zhang, TF Lue; (II) Administrative support: G Lin, L Banie; (III) Provision of study materials or patients: G Lin, M Van Kuiken, G Wang, L Banie, Y Tan, F Zhou, Z Wang, Y Chen; (IV) Collection and assembly of data: G Lin, G Wang, L Banie, Y Tan, F Zhou, Z Wang, Y Chen; (V) Data analysis and interpretation: G Lin, M Van Kuiken, G Wang, L Banie, Y Tan, F Zhou, Z Wang, Y Chen, TF Lue; (VI) Manuscript writing: All authors; (VII) Final approval of manuscript: All authors.

Correspondence to: Tom F. Lue, MD. Knuppe Molecular Urology Laboratory, Department of Urology, School of Medicine, University of California, San Francisco, CA 94143-0738, USA. Email: tom.lue@ucsf.edu.

Background: The mechanisms of the microenergy acoustic pulse (MAP) therapy on restoring structure and function of pelvic floor muscles (PFM) after simulated birth injury are not well understood.

Methods: A total 24 female Sprague-Dawley rats were randomly grouped into sham control (sham), vaginal balloon dilation and ovariectomy (VBDO), VBDO + β-aminopropionitrile (BAPN, an irreversible LOX inhibitor), and VBDO + BAPN and treated with MAP (n=6 in each group). The MAP therapy was administered 2 times per week for 4 weeks with 1-week washout, the functional and histological studies were conducted in all 24 rats. The viscoelastic behavior of the PFM, including iliococcygeus (IC) and pubococcygeus (PC), was examined with a biomechanical assay. The structure of the PFM was assessed by immunofluorescence and Masson's trichrome staining.

Results: The leak point pressure (LPP) assay demonstrated that the MAP therapy group had higher LPPs compared to that of VBDO and BAPN groups. In the sham group, the muscular stiffness (K) of IC muscle was significantly higher than that of PC muscle while the pelvic floor muscle rebound activity (MRA) of PC muscle was stronger than that of IC muscle (291.26 ± 45.33 and 241.18 ± 14.23 N/cm^2, respectively). Both VBDO and BAPN decreased the MRA and increased the K in both IC and PC. Histologic examination revealed increased fibrous tissue (collagen) and degeneration of muscle fibers in both VBDO and BAPN groups. MAP therapy significantly reduced the collagen content and improved the architecture of muscle fibers.

Conclusions: MAP appears to restore the structure and function of PFM by regenerating muscular fibers and improving biomechanical properties in an animal model of simulated birth injury.

Keywords: Microenergy acoustic pulses (MAP); pelvic floor muscles (PFM); stress urinary incontinence (SUI); vaginal balloon dilation and ovariectomy (VBDO); β-aminopropionitrile (BAPN)

Introduction

Stress urinary incontinence (SUI) affects about 167 million women worldwide (a prevalence of 3.3%) (1,2), with 45.9% of women in the United States reporting symptoms of SUI (3). Furthermore, pelvic organ prolapse (POP) has an estimated prevalence of 3–6%, and as high as 50% when evaluated based on vaginal examination alone (1,4). Non-surgical treatment options for SUI and POP include the

exercises of pelvic floor muscle, electric stimulation, and creams with different hormones. While these conservative therapies are pretty safe, the durability and efficacy are limited. In the US, the mainstay of surgical treatment for SUI is the mid-urethral sling, but can also include autologous fascial pubovaginal slings, urethral bulking, or colposuspension. For symptomatic POP, surgical procedures include repair with native tissue, abdominal sacrocolpopexy, and transvaginal mesh. Currently, the surgeries with meshes for both SUI and POP are very effective, but mesh exposure, infection, severe pelvic pain, and the dyspareunia are complications in the clinic. In the United States alone, those clinical complications have resulted in more than 140,000 lawsuits, and the complete cessation of transvaginal mesh kits for POP has been issued in the USA (5), in Australia, and in UK. At the same time, from July 2018, the mesh surgeries for SUI were also stopped in UK.

Awareness of mesh-related complications, interest in applying regenerative medicine approaches to restore the structure and function of urethral sphincter and pelvic floor was increased (6-10). Currently, the stem cell therapy for SUI is dominated (11-13), as well as the tissue engineering associated with stem cells for POP (14). However, extensive investigation before its clinical application is needed. Very recently, using products related to stem cells and the tissue-resident stem/progenitor cells (15,16) to enhance the regeneration process is another research hot topic (10,17-19).

The pathophysiology of pelvic floor disorders (PFDs) such as SUI and POP is still unclear, but it has been demonstrated that involves genetic susceptibility, connective tissue abnormal, hormone effects, obesity, pregnancy, hysterectomy, constipation, and advanced age (20). It has been demonstrated that pelvic floor muscle dysfunction is a key factor in the development of PFDs. However, as muscle physiologists tend to study the behavior of contracting muscles, this focus on muscle contraction means that the research on the mechanical properties of relaxing muscles has been relatively neglected. The passive properties of muscles play a central role in various physiological and pathophysiological processes (21,22) and merit more attention and research (23,24).

Many studies using low-energy shock waves on other organs have been published (25,26). However, there are limited studies on the mechanobiological effects of the microenergy acoustic pulses (MAP) which is a modified low-intensity shock wave with a different wave form, on the bladder, urethra, and pelvic floor muscles (PFM) (27-30). In current study, we propose to further elucidate the molecular mechanisms involved.

This study aims to measure the passive biomechanical properties of PFM because the biomechanical properties of PFM affect their stretching range and position. In this current study, a stress-relaxation test on fresh rat pelvic floor muscle tissue was conducted, and the effects of MAP therapy on the structure and function of PFM was assessed. The following article is presented in accordance with the ARRIVE reporting checklist (available at https://tau.amegroups.com/article/view/10.21037/tau-22-30/rc).

Methods

Experimental animals and design

Experiments were performed under a project license (No. AN187720) granted by ethics board of the Institutional Animal Care and Use Committee at the University of California, San Francisco, in compliance with the guidelines for the care and use of animals. A total 24 female Sprague-Dawley rats at 12 weeks old were purchased from Charles River Laboratories (Wilmington, MA, USA), and randomly grouped into 4 including the sham control (sham) group, vaginal balloon dilation and ovariectomy (VBDO) group, VBDO and β-aminopropionitrile (BAPN) group, and VBDO plus BANP treated with MAP twice a week for 4 weeks (MAP group). The VBDO procedure was performed as reported (31). Briefly, under the anesthesia with ketamine/xylazine, an 18 Fr Foley catheter was placed into the rat's vagina, and the balloon was subsequently filled with 4 mL water. A constant pull to direct the force to the pelvic floor of 130-g weight was placed on the suspended end of the catheter, which was left in place for 4 hours. Seven days later, bilateral ovaries were removed. All animals in the BAPN and MAP groups received 300 mg/kg of BAPN (intraperitoneal injections, twice a week for 4 weeks), and the rats in MAP groups were then treated with MAP. After 1 week of wash-out post the last MAP treatment, the leak point pressure (LPP) was measured in all rats. The rats were sacrificed and the PFM were harvested for muscular biomechanical and histological study (Figure S1).

MAP therapy

A compact electromagnetic unit as acoustic pulse source of MAP was applied (LiteMed Inc., Taipei). To overlay the

area of the urethra and pelvis, the MAP probe was coupled to the skin by using ultrasound gel (Aquasonic, Parker Laboratories Inc., Fairfield, NJ, USA) and targeted to the pelvis of rat. The energy flux density was 0.033 mJ/mm^2, 500 pulses at 3 Hz. The MAP treatment was conducted twice a week for 4 weeks. The LPP measurement were performed after 1-week wash-out in all rats followed by sacrifice and tissue harvest for histological studies.

Urethral LPP assay

The urethral LPP was assessed as described previously (32). Briefly, with the anesthesia of urethane, a tube (polyethylene-90) was placed into the bladder dome. The bladder volume was recorded by slowly filling with warmed phosphate buffered saline (PBS), which was repeated 3 times to obtain the average bladder capacity. The bladder was then emptied via aspiration and manual pressure. A 40% of bladder capacity was then filled and increasing manual extravesical pressure was applied until leakage was noted. The intravesical pressure changes were recorded by a computer with LabView 6.0 software (National Instruments, Austin, TX, USA). In general, this procedure was repeated six times to get average LPPs.

Ex vivo pelvic floor muscle biomechanical assays

The PFM, including iliococcygeus (IC) and pubococcygeus (PC) (33,34), were harvested from experimental animals to determine parameters describing their structural properties. The viscoelastic behavior of pelvic floor muscle was checked with a biomechanical assay. A stress-strain curve was generated by applying the pelvic floor muscle strip on the Force Transducer Head of 400B series of high-level output force transducers (Aurora Scientific, Aurora, ON, Canada) (Figure S2) (23). In brief, the muscle strips of PC and IC were applied on the hook of force sensor and length controller. The muscle strip was kept at equilibrium for 5 minutes before and between each force was applied. A maximum force of 330 gm was applied to each muscle strip and the force was held constantly. Then the muscular creep phenomenon was measured and recorded with Myobath Tissue Bath System II (World Precision Instruments, Sarasota, FL, USA). The muscle rebound activity (MRA) was calculated with following equation: MRA (N/cm^2) = [force (g) × muscle length (cm) ×1.06]/[muscle weight (g) ×0.00981] (35).

In addition, the elastic region and plastic region of the pelvic floor muscle stress-strain curve were also analyzed. The muscular flexibility can be measured by calculating the muscular stiffness (K), which is defined as the extent to which an object resists deformation in response to an applied force. In general, the more flexible an object is, the less stiff it is (36). The equation for K is: K = F/δ (37). F is the force on the pelvic floor muscle, δ is the displacement produced by the force long the same degree of freedom of the pelvic floor muscle. A fixed 330 gm stress stimulus was applied to the muscle strip, and then left to bounce back on its own. The stress-relaxation curve of the muscle bounce-back within 2 minutes was recorded with Myobath Tissue Bath System II. The time for muscle rebound of 60 gm force from the limit point 300 gm stress stimulus was recorded, and the K was calculated. Differences among groups were statistically analyzed.

Immunofluorescence staining and Masson's trichrome stain

Tissue samples were fixed and embedded in OCT Compound (Sakura Finetic USA, Torrance, CA, USA) and tissue section were made. The tissues slides were incubated overnight at 4 ℃ with primary antibodies for Laminin (1:500; Abcam, Waltham, MA, USA). Control tissue sections were similarly prepared except no primary antibody was added and followed by secondary antibody conjugated with Alexa-594 (1:500; Invitrogen, Carlsbad, CA, USA). The Alexa-488-conjugated phalloidin (1:500; Invitrogen) was used to stain muscle fiber. The tissues were then stained with 4',6-diamidino-2-phenylindole (DAPI, for nuclear staining, 1 µg/mL, Sigma-Aldrich, St. Louis, MO, USA) followed imaging with fluorescence microscopy. Five randomly selected fields per tissue were photographed and recorded using a Retiga Q Image digital still camera and analyzed with ACT-1 software (Nikon Instruments Inc., Melville, NY, USA).

Statistical analysis

The current results were analyzed using GraphPad Prism version 5.0 (GraphPad Software, San Diego, CA, USA) and expressed as mean ± standard error of the mean. One-way analysis of variance followed by the Tukey's post hoc test for multiple comparisons were performed, while the differences were considered significant at $P<0.05$.

Results

MAP therapy improved urethral LPP

In general, the urethral injury recovered quickly in the VBDO animal model. Urethral LPP in VBDO alone (34.6 ± 1.8 cmH$_2$O) recovered more than that in BAPN group (28.2 ± 4.2 cmH$_2$O), but both significantly lower than sham group (57.3 ± 8 cmH$_2$O) (n=6, P<0.05). BAPN is an irreversible LOX inhibitor that affects the crosslinking of collagen and elastin. Therefore, after BAPN treatment, the urethral injury is difficult to recover. Our results showed that even at the 10th week after the injury, the urethral LPP was still significantly lower than the sham and VBDO groups. Compared to the VBDO and BAPN groups, application of MAP therapy significantly improved the LPP to 52.8 ± 8.4 cmH$_2$O (P<0.05).

Effect of MAP therapy on pelvic floor muscle biomechanical properties

The PFM are the dominate tissues that bear the weight of pelvic organs and intra-abdominal pressure. Therefore, in addition to muscular contraction and relaxation, the static mechanical properties of PFM are very important. The biomechanical properties of PFM include muscle stiffness, flexibility, and ability to rebound. In order to determine these characteristics of the PFM, we carefully dissected PC and IC muscular strips, the stress-relaxation curve was recorded via the 400B series of high-level output force transducers (Aurora Scientific) (Figure S2). The K coefficient and the MRA were then calculated. Our results showed thicker endomysium and perimysium in IC than PC muscle, which may explain the higher K coefficient of IC muscle than that of PC muscle. This trend is similar in all groups (*Figure 1*).

In regard to MRA, the PC muscles have stronger rebound force than that of IC, 291.26 ± 45.33 and 241.18 ± 14.23 N/cm^2, respectively. The VBDO significantly decreased the MRA of both PC (227.79 ± 93.35 N/cm^2) and IC (211.99 ± 86.88 N/cm^2). BAPN also decreased the rebound force in both PC (219.44 ± 29.94 N/cm^2) and IC (182.07 ± 51.78 N/cm^2). The MAP treatment significantly improved the muscle rebound force of PC and IC (381.20 ± 52.95 and 371.17 ± 40.47 N/cm^2, respectively), and both are higher than the sham group (*Figure 2*).

In terms of K coefficient, VBDO increased the stiffness of PC muscles, and the addition of BAPN further aggravated this increase in stiffness. The MAP treatment

improved the K coefficient, but not to the level of the normal control (*Figure 3*). In IC muscles, the increase of K coefficient by VBDO and BAPN is more pronounced. Similarly, MAP treatment improved the K coefficient, but not to normal control levels (*Figure 4*).

MAP therapy restored pelvic floor muscle structure

In the trichrome staining of the PFM, there was an increase in collagen fibers seen between the muscle fibers in both the VBDO and BAPN groups, however, MAP therapy significantly reduced the amount of collagen fibers seen (*Figure 5*). In addition, there were also disrupted muscles and muscular sarcolemma along with irregularly arranged muscle fibers in both VBDO and BAPN groups. In longitudinal sections, the muscle fibers became curly and segmented, and the spaces between the muscle fibers became larger and irregular. In cross sections, the muscle fibers appeared atrophied and thinner, and the spaces between the muscles fibers also became wider. Moreover, deficiency of endomysium and perimysium with disorganized muscle fibers were noted in both VBDO and BAPN group while MAP therapy partially restored the structural integrity (*Figure 6*).

Discussion

The PFM are an important factor in maintaining the structural integrity and function of the pelvic floor (24). Many recent studies have found that pelvic floor muscle dysfunction can lead to SUI (38), POP and fecal incontinence (39), as well as sexual dysfunction (40).

In preclinical studies, we have applied MAP therapy to vaginal balloon dilation-induced and obesity-associated SUI with excellent results. We have shown that the tissue-resident stem cells within PFM can be activated to regenerate PFM and improve SUI (27,41). We have published methods to isolate CD45$^-$/CD11b$^-$/CD31$^-$/Sca1$^-$/CD34$^+$/integrin-α7$^+$ striated muscle stem/progenitor cells from PFM and demonstrated the activation of those cells by MAP with FACS assay (42).

Although we have demonstrated in two animal models that PFM can be regenerated using MAP treatment, the biomechanical function of the PFM after regeneration has not been studied *in vitro* (41,43). In this current study, we applied biomechanical measurement technology to examine stress-relaxation curves and conducted an in-depth study on the MRA and K coefficient. We found that the MRA of
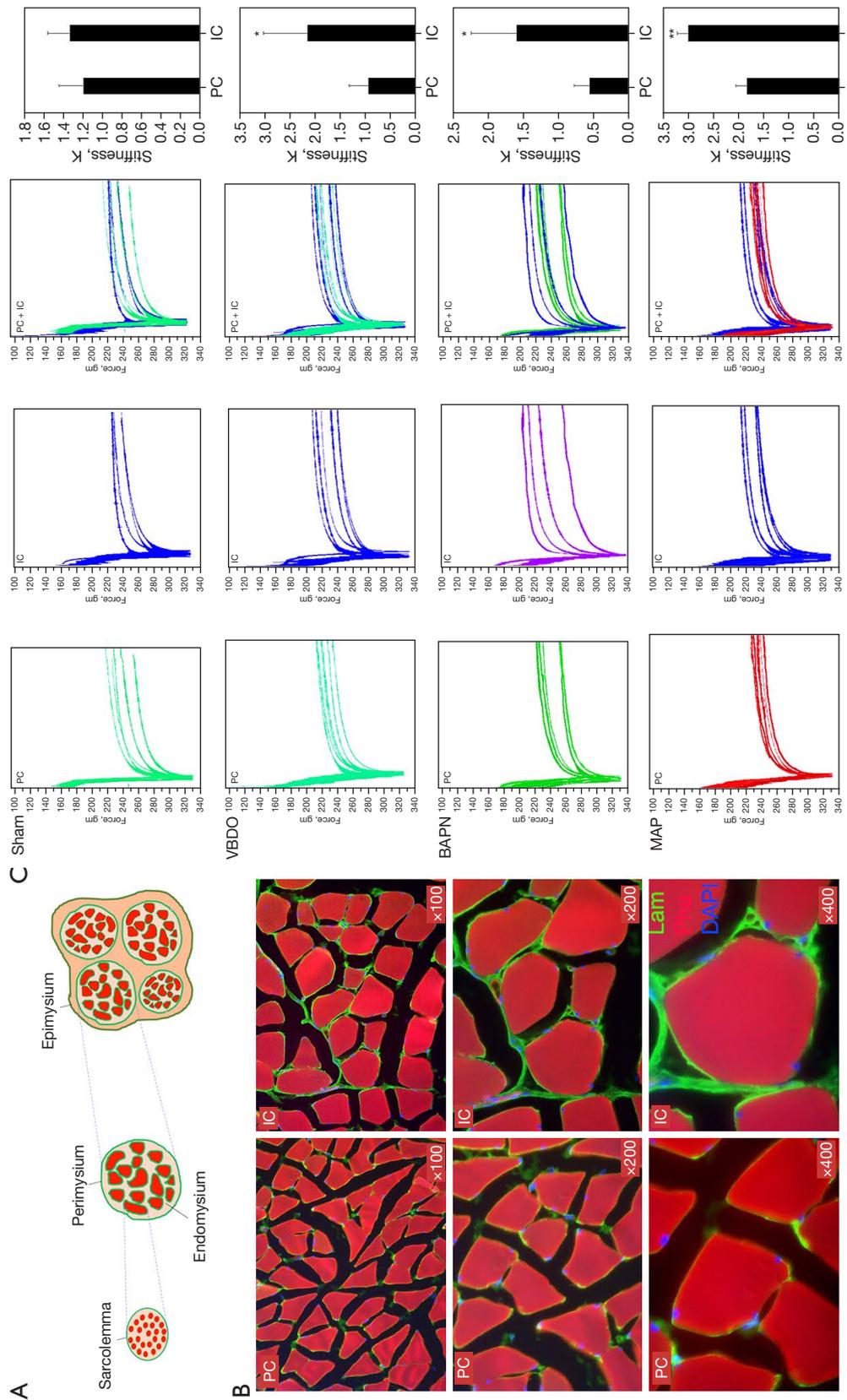
Figure 1 Difference of muscle stiffness between PC and IC. (A) The diagram depicts the muscle fibers, endomysium, perimysium, epimysium and sarcolemma. (B) IC muscle fibers have thicker endomysium and perimysium than the PC muscle fibers (Laminin: green; Phalloidin: red; DAPI: blue). Magnification: ×100, ×200, ×400. (C) Muscle stress-relaxation curve of PC and IC in 4 groups: sham, VBDO, BAPN and MAP. Muscle stiffness of in 4 groups: sham, VBDO, BAPN and MAP. The bar chart represented the average muscle stiffness coefficient of PC and IC muscle in four groups (n=6; *, P<0.05, compared with PC; **, P<0.01). PC, pubococcygeus; IC, iliococcygeus; DAPI, 4′,6-diamidino-2-phenylindole; VBDO, vaginal balloon dilation and ovariectomy; BAPN, β-aminopropionitrile; MAP, microenergy acoustic pulse.
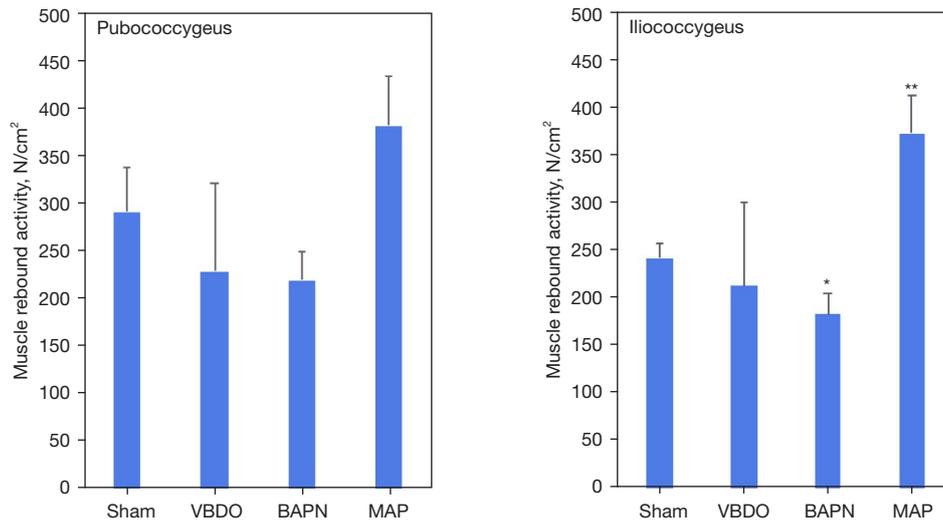
Figure 2 MRA affected by MAP in rats. Average MRA of the 4 groups: sham, VBDO, BAPN and MAP in both PC and IC (n=6; *, P<0.05, compared with the sham group; **, P<0.01, compared with the VBDO and BAPN group). VBDO, vaginal balloon dilation and ovariectomy; BAPN, β-aminopropionitrile; MAP, microenergy acoustic pulse; MRA, muscle rebound activity; PC, pubococcygeus; IC, iliococcygeus.
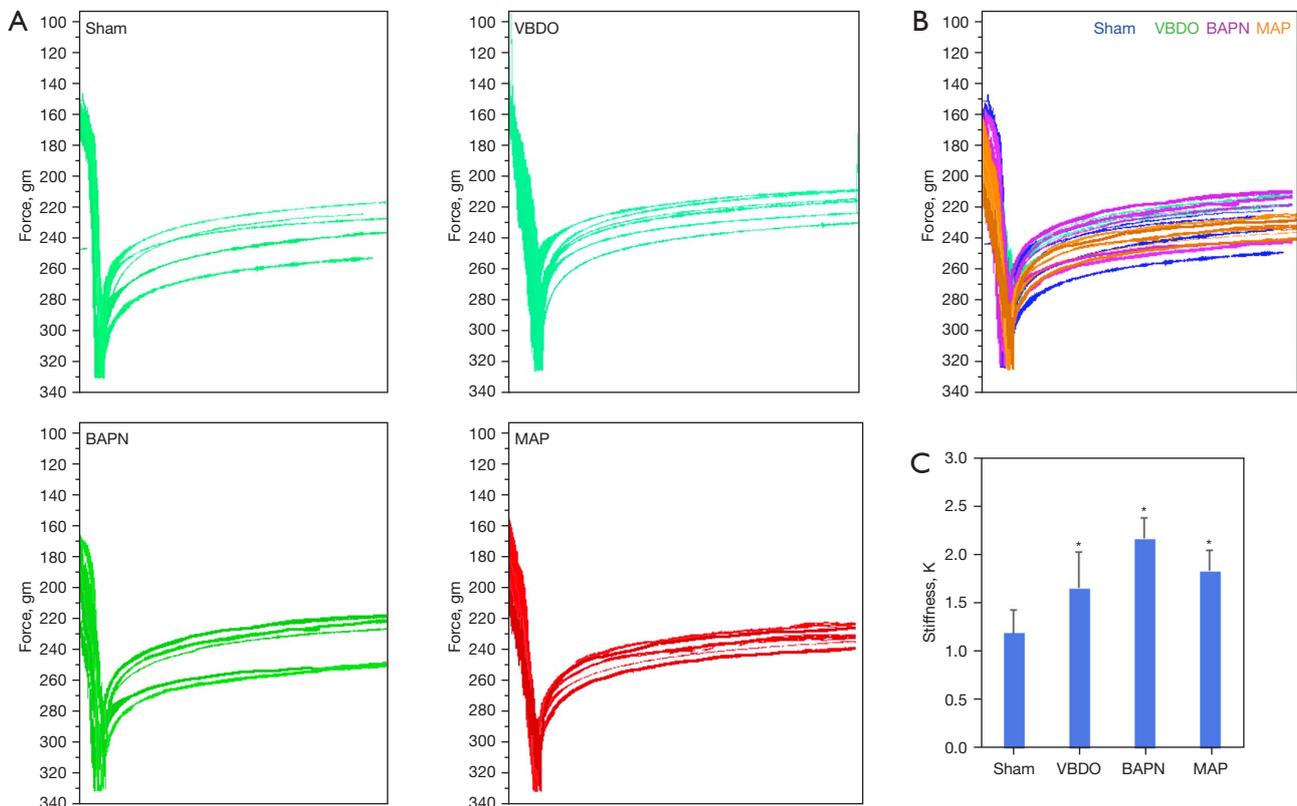

Figure 3 PC muscle stiffness affected by MAP in rats. (A) The stress-relaxation curve of each PC trips in 4 groups: sham, VBDO, BAPN and MAP. (B) Merged stress-relaxation curve of each PC trips from all four groups. (C) Average PC muscle stiffness coefficient in four groups (n=6; *, P<0.05, compared with the sham group). VBDO, vaginal balloon dilation and ovariectomy; BAPN, β-aminopropionitrile; MAP, microenergy acoustic pulse; PC, pubococcygeus.
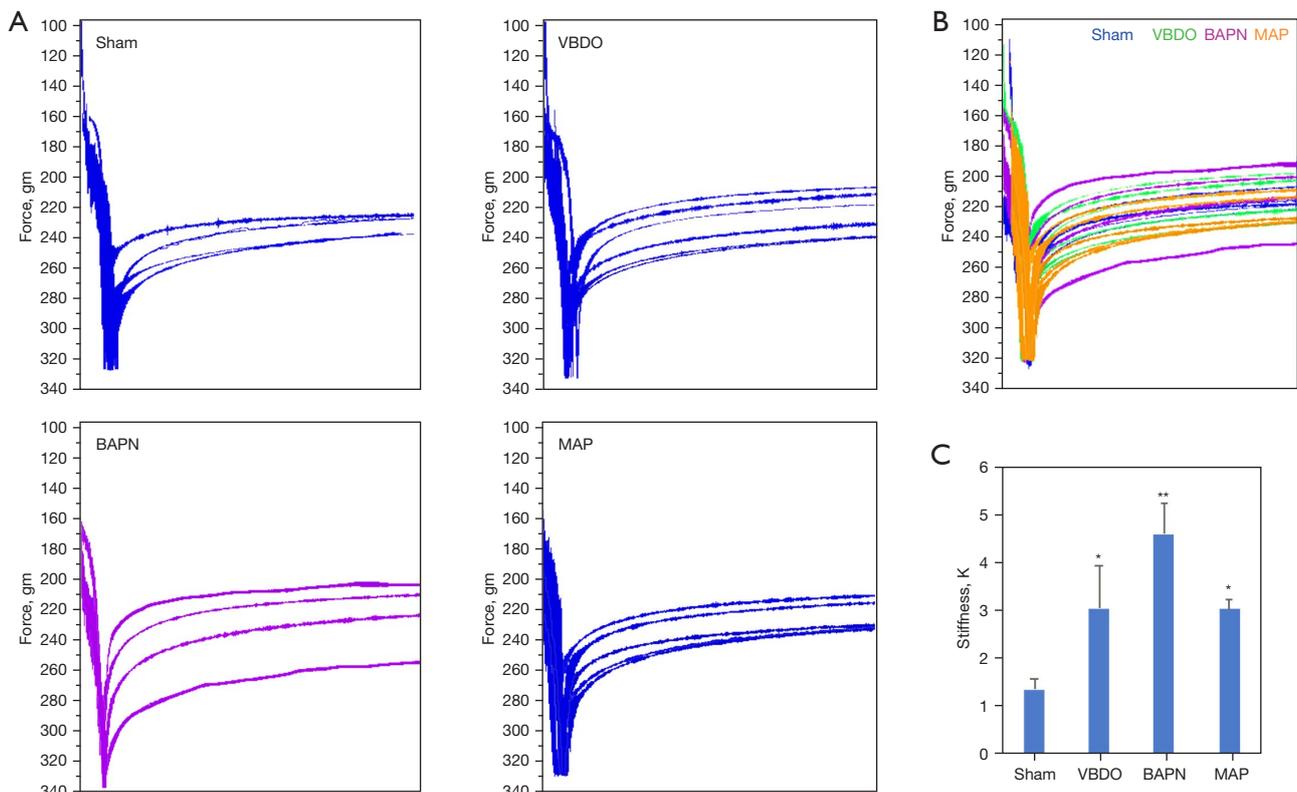
Figure 4 IC muscle stiffness affected by MAP in rats. (A) The stress-relaxation curve of each PC trips in 4 groups: sham, VBDO, BAPN and MAP. (B) Merged stress-relaxation curve of each PC trips from all four groups. (C) Average PC muscle stiffness coefficient in four groups (n=6; *, P<0.05, compared with the sham group; **, P<0.01). VBDO, vaginal balloon dilation and ovariectomy; BAPN, β-aminopropionitrile; MAP, microenergy acoustic pulse; IC, iliococcygeus; PC, pubococcygeus.

PC is higher than that of IC, while stiffness of IC muscle is significantly higher than that of PC. These results imply that PC may play a more prominent role in contraction and relaxation, while IC maintains static support of pelvic floor.

Our current results also showed significantly improved rebound forces of both IC and PC muscles after MAP therapy, indicating that muscle fibers have been regenerated and function restored. In addition, MAP therapy also decreased muscle stiffness and improved muscle flexibility. These changes in IC are significantly higher than the changes in PC.

Our current research also found that the damaged and degenerated pelvic floor muscle fibers were restored after MAP treatment. This has also been reported in our previous publications (27,41,43). In 2017, we isolated the urethral striated muscle-derived stem cells (uMDSCs) and differentiated those cells into myotubes *in vitro* (42). In our recent study, we demonstrated that MAP-treated

muscle derived stem cells have increased expression of myosin heavy chain (MHC) and myogenin (Myo G) (44). We also studied the signaling pathways that propel the MAP-enhanced formation of myotubes from rat L6 myoblast cells, and tentatively identified that both protein kinase RNA-like endoplasmic reticulum kinase/Activating Transcription Factor 4 (PERK/ATF4) and Wnt-β-catenin signaling pathways are involved in these processes (45).

Regarding the changes in the stiffness of the PFM, our results demonstrated increased amount of collagen fibers within the PFM in the animals treated with VBDO and BAPN, which leads to an increase in muscle stiffness, i.e., a decrease in muscle flexibility. MAP therapy significantly reduced the collagen fibers between muscles fibers, which may explain the decrease in stiffness of the PFM after MAP treatment. We have not studied the mechanisms involved in the reduction of interstitial collagen between muscle fibers after MAP therapy. Nevertheless, low-intensity
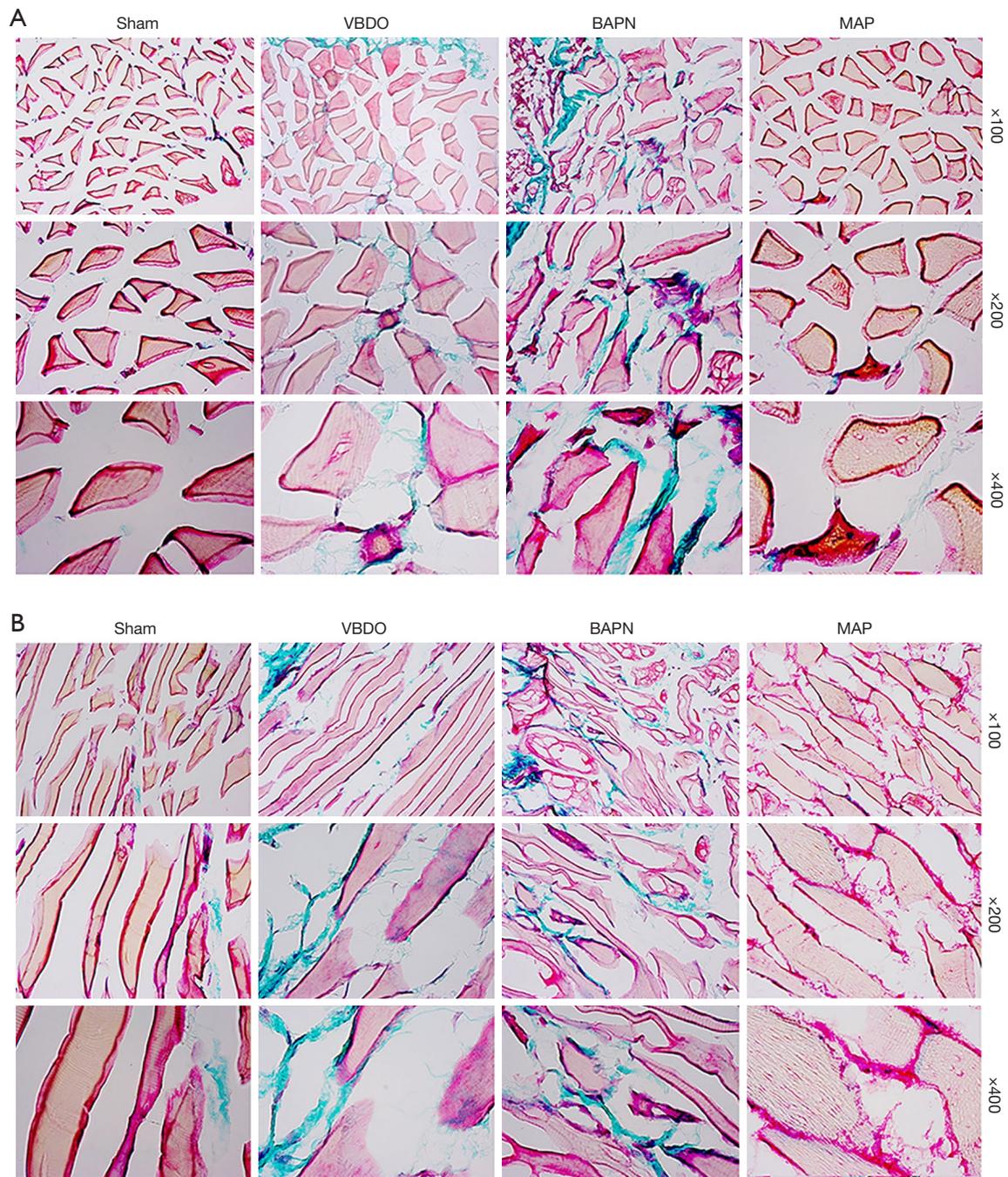
　　　　Transl Androl Urol 2022;11(5):595-606 | https://dx.doi.org/10.21037/tau-22-30

Figure 5 Effect of MAP on extracellular matrix within pelvic floor muscle. (A) Representative cross sections of PFM stained by Trichrome staining in four groups: sham, VBDO, BAPN and MAP. Magnification: ×100, ×200, ×400. (B) Representative longitude section of PFM stained by Trichrome staining in four groups. Magnification: ×100, ×200, ×400. There are more interstitial collagen fibers in both VBDO and BAPN groups. VBDO, vaginal balloon dilation and ovariectomy; BAPN, β-aminopropionitrile; MAP, microenergy acoustic pulse; PFM, pelvic floor muscles.
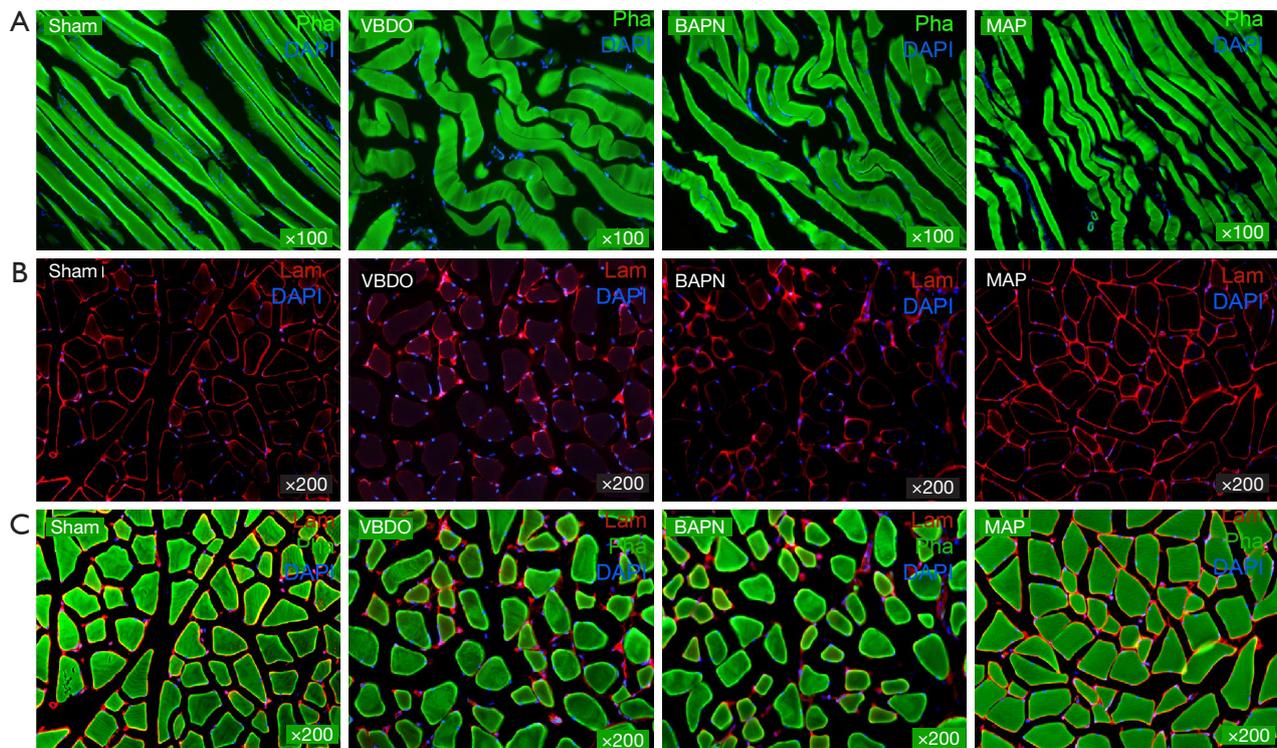
Transl Androl Urol 2022;11(5):595-606 | https://dx.doi.org/10.21037/tau-22-30

Figure 6 MAP partially restored the integrity of PFM damaged by VBDO and BAPN. Female adult rats VBDO and BAPN injections (VBDO + BAPN), with or without MAP therapy. Sham surgery was performed in the control group (sham) (n=6 in each group). The PC muscle was harvested for histology. Antibodies/chemicals used: Phalloidin for muscle (Pha, green), Laminin (Lam, red) for sarcolemma, DAPI for cell nuclei (blue). (A) Longitudinal sections of striated muscle fiber (×100). (B,C) Cross sections (×200). Deficiency of endomysium and perimysium with disorganized muscle fibers were noted in both VBDO and BAPN group while MAP partially restored the muscle integrity. DAPI, 4',6-diamidino-2-phenylindole; VBDO, vaginal balloon dilation and ovariectomy; BAPN, β-aminopropionitrile; MAP, microenergy acoustic pulse; PFM, pelvic floor muscles; PC, pubococcygeus.

extracorporeal shock wave therapy (Li-ESWT)-induced reduction of collagen fibers in liver fibrosis and spine surgery has been attributed to modulation of the TGF-signaling pathway and matrix metalloproteinases (46,47).

Our current study is the first to examine the biomechanical effects of MAP on the PFM after simulated birth injury. We have reported differential results in IC and PC muscles. However, the correlation between the contraction and relaxation function and the mechanical biomechanics of the pelvic floor muscle has not been determined. Further studies are warranted.

Conclusions

MAP therapy appears to restore the structure and function of pelvic floor muscle in female rats by regenerating the muscular fibers and improving muscular biomechanical

properties. Our results suggest that MAP therapy may be a non-invasive therapeutic approach for PFDs such as SUI and POP.

Footnote

Reporting Checklist: The authors have completed the

604

Lin et al. MAP restore function and structure of PFM

ARRIVE reporting checklist. Available at https://tau.amegroups.com/article/view/10.21037/tau-22-30/rc

Data Sharing Statement: Available at https://tau.amegroups.com/article/view/10.21037/tau-22-30/dss

Conflicts of Interest: All authors have completed the ICMJE uniform disclosure form (available at https://tau.amegroups.com/article/view/10.21037/tau-22-30/coif). TFL serves as an unpaid Editor-in-Chief for *Translational Andrology and Urology*. GL serves as an unpaid Editorial Board Member from August 2020 to July 2022 for *Translational Andrology and Urology*. YZ is the founder and CEO of HillMed Inc. and BrainHealth Tech Inc. TFL is a consultant, co-founder and investor of Acoustic Wave Cell Therapy, Inc. The other authors have no conflicts of interest to declare.

Ethical Statement: The authors are accountable for all aspects of the work in ensuring that questions related to the accuracy or integrity of any part of the work are appropriately investigated and resolved. Experiments were performed under a project license (No. AN187720) granted by ethics board of the Institutional Animal Care and Use Committee at the University of California, San Francisco, in compliance with the institutional guidelines for the care and use of animals.

Open Access Statement: This is an Open Access article distributed in accordance with the Creative Commons Attribution-NonCommercial-NoDerivs 4.0 International License (CC BY-NC-ND 4.0), which permits the non-commercial replication and distribution of the article with the strict proviso that no changes or edits are made and the original work is properly cited (including links to both the formal publication through the relevant DOI and the license). See: https://creativecommons.org/licenses/by-nc-nd/4.0/.

References

1. D'Angelo W, Dziki J, Badylak SF. The challenge of stress incontinence and pelvic organ prolapse: revisiting biologic mesh materials. Curr Opin Urol 2019;29:437-42.
2. Irwin DE, Kopp ZS, Agatep B, et al. Worldwide prevalence estimates of lower urinary tract symptoms, overactive bladder, urinary incontinence and bladder outlet obstruction. BJU Int 2011;108:1132-8.
3. Abufaraj M, Xu T, Cao C, et al. Prevalence and trends in urinary incontinence among women in the United States, 2005-2018. Am J Obstet Gynecol 2021;225:166.e1-166.e12.
4. Barber MD, Maher C. Apical prolapse. Int Urogynecol J 2013;24:1815-33.
5. FDA. Urogynecologic Surgical Mesh Implants. 2019. Available online: https://www.fda.gov/medical-devices/implants-and-prosthetics/urogynecologic-surgical-mesh-implants
6. Shamliyan TA, Kane RL, Wyman J, et al. Systematic review: randomized, controlled trials of nonsurgical treatments for urinary incontinence in women. Ann Intern Med 2008;148:459-73.
7. Chermansky CJ, Winters JC. Complications of vaginal mesh surgery. Curr Opin Urol 2012;22:287-91.
8. Kirchin V, Page T, Keegan PE, et al. Urethral injection therapy for urinary incontinence in women. Cochrane Database Syst Rev 2012;(2):CD003881.
9. Vinarov A, Atala A, Yoo J, et al. Cell therapy for stress urinary incontinence: Present-day frontiers. J Tissue Eng Regen Med 2018;12:e1108-21.
10. Bennington J, Williams JK, Andersson KE. New concepts in regenerative medicine approaches to the treatment of female stress urinary incontinence. Curr Opin Urol 2019;29:380-4.
11. Lin CS, Lue TF. Stem cell therapy for stress urinary incontinence: a critical review. Stem Cells Dev 2012;21:834-43.
12. Gill BC, Damaser MS, Vasavada SP, et al. Stress incontinence in the era of regenerative medicine: reviewing the importance of the pudendal nerve. J Urol 2013;190:22-8.
13. Thaker H, Sharma AK. Regenerative medicine based applications to combat stress urinary incontinence. World J Stem Cells 2013;5:112-23.
14. Chapple CR, Osman NI, Mangera A, et al. Application of Tissue Engineering to Pelvic Organ Prolapse and Stress Urinary Incontinence. Low Urin Tract Symptoms 2015;7:63-70.
15. Blau HM, Daley GQ. Stem Cells in the Treatment of Disease. N Engl J Med 2019;380:1748-60.
16. Zambon JP, Williams KJ, Bennington J, et al. Applicability of regenerative medicine and tissue engineering for the treatment of stress urinary incontinence in female patients. Neurourol Urodyn 2019;38 Suppl 4:S76-83.
17. Aufderklamm S, Aicher WK, Amend B, et al. Stress urinary incontinence and regenerative medicine: is injecting functional cells into the urethra feasible based on current knowledge and future prospects? Curr Opin Urol 2019;29:394-9.

18. Yan H, Zhong L, Jiang Y, et al. Controlled release of insulin-like growth factor 1 enhances urethral sphincter function and histological structure in the treatment of female stress urinary incontinence in a rat model. BJU Int 2018;121:301-12.

19. Koudy Williams J, Dean A, Lankford S, et al. Efficacy and Initial Safety Profile of CXCL12 Treatment in a Rodent Model of Urinary Sphincter Deficiency. Stem Cells Transl Med 2017;6:1740-6.

20. Couri BM, Lenis AT, Borazjani A, et al. Animal models of female pelvic organ prolapse: lessons learned. Expert Rev Obstet Gynecol 2012;7:249-60.

21. Herbert RD, Gandevia SC. The passive mechanical properties of muscle. J Appl Physiol (1985) 2019;126:1442-4.

22. Nagle AS, Barker MA, Kleeman SD, et al. Passive biomechanical properties of human cadaveric levator ani muscle at low strains. J Biomech 2014;47:583-6.

23. Van Loocke M, Lyons CG, Simms CK. Viscoelastic properties of passive skeletal muscle in compression: stress-relaxation behaviour and constitutive modelling. J Biomech 2008;41:1555-66.

24. Catanzarite T, Bremner S, Barlow CL, et al. Pelvic muscles' mechanical response to strains in the absence and presence of pregnancy-induced adaptations in a rat model. Am J Obstet Gynecol 2018;218:512.e1-9.

25. Gruenwald I, Appel B, Vardi Y. Low-intensity extracorporeal shock wave therapy--a novel effective treatment for erectile dysfunction in severe ED patients who respond poorly to PDE5 inhibitor therapy. J Sex Med 2012;9:259-64.

26. Vardi Y, Appel B, Kilchevsky A, et al. Does low intensity extracorporeal shock wave therapy have a physiological effect on erectile function? Short-term results of a randomized, double-blind, sham controlled study. J Urol 2012;187:1769-75.

27. Wu AK, Zhang X, Wang J, et al. Treatment of stress urinary incontinence with low-intensity extracorporeal shock wave therapy in a vaginal balloon dilation induced rat model. Transl Androl Urol 2018;7:S7-16.

28. Lin G, Reed-Maldonado AB, Wang B, et al. In Situ Activation of Penile Progenitor Cells With Low-Intensity Extracorporeal Shockwave Therapy. J Sex Med 2017;14:493-501.

29. Ruan Y, Zhou J, Kang N, et al. The effect of low-intensity extracorporeal shockwave therapy in an obesity-associated erectile dysfunction rat model. BJU Int 2018;122:133-42.

30. Liu T, Shindel AW, Lin G, et al. Cellular signaling

pathways modulated by low-intensity extracorporeal shock wave therapy. Int J Impot Res 2019;31:170-6.

31. Wang G, Lin G, Zhang H, et al. Effects of prolonged vaginal distension and β-aminopropionitrile on urinary continence and urethral structure. Urology 2011;78:968.e13-9.

32. Wang L, Lin G, Lee YC, et al. Transgenic animal model for studying the mechanism of obesity-associated stress urinary incontinence. BJU Int 2017;119:317-24.

33. Jiang HH, Salcedo LB, Song B, et al. Pelvic floor muscles and the external urethral sphincter have different responses to applied bladder pressure during continence. Urology 2010;75:1515.e1-7.

34. Gómez YC, Jiang H, Zaszczurynski P, et al. Electromyography of Pelvic Floor Muscles in Rats. In: Mizrahi J. editor. Advances in Applied Electromyography. London: IntechOpen, 2011.

35. Lee YC, Lin G, Wang G, et al. Impaired contractility of the circular striated urethral sphincter muscle may contribute to stress urinary incontinence in female zucker fatty rats. Neurourol Urodyn 2017;36:1503-10.

36. Haussler KK, Martin CE, Hill AE. Efficacy of spinal manipulation and mobilisation on trunk flexibility and stiffness in horses: a randomised clinical trial. Equine Vet J Suppl 2010;(38):695-702.

37. Baumgart E. Stiffness--an unknown world of mechanical science? Injury 2000;31 Suppl 2:S-B14-23.

38. Lawrence JM, Lukacz ES, Liu IL, et al. Pelvic floor disorders, diabetes, and obesity in women: findings from the Kaiser Permanente Continence Associated Risk Epidemiology Study. Diabetes Care 2007;30:2536-41.

39. Chan KYC, Suen M, Coulson S, et al. Efficacy of pelvic floor rehabilitation for bowel dysfunction after anterior resection for colorectal cancer: a systematic review. Support Care Cancer 2021;29:1795-809.

40. Verbeek M, Hayward L. Pelvic Floor Dysfunction And Its Effect On Quality Of Sexual Life. Sex Med Rev 2019;7:559-64.

41. Zhang X, Ruan Y, Wu AK, et al. Delayed Treatment With Low-intensity Extracorporeal Shock Wave Therapy in an Irreversible Rat Model of Stress Urinary Incontinence. Urology 2020;141:187.e1-7.

42. Wang B, Ning H, Reed-Maldonado AB, et al. Low-Intensity Extracorporeal Shock Wave Therapy Enhances Brain-Derived Neurotrophic Factor Expression through PERK/ATF4 Signaling Pathway. Int J Mol Sci 2017;18:433.

43. Yuan H, Ruan Y, Tan Y, et al. Regenerating Urethral

Transl Androl Urol 2022;11(5):595-606 | https://dx.doi.org/10.21037/tau-22-30

Striated Muscle by CRISPRi/dCas9-KRAB-Mediated Myostatin Silencing for Obesity-Associated Stress Urinary Incontinence. CRISPR J 2020;3:562-72.

44. Cui K, Kang N, Banie L, et al. Microenergy acoustic pulses induced myogenesis of urethral striated muscle stem/progenitor cells. Transl Androl Urol 2019;8:489-500.

45. Wang B, Zhou J, Banie L, et al. Low-intensity extracorporeal shock wave therapy promotes myogenesis through PERK/ATF4 pathway. Neurourol Urodyn

2018;37:699-707.

46. Haberal B, Şimşek EK, Akpınar K, et al. Impact of radial extracorporeal shock wave therapy in post-laminectomy epidural fibrosis in a rat model. Jt Dis Relat Surg 2021;32:162-9.

47. Ujiie N, Nakano T, Yamada M, et al. Low-energy extracorporeal shock wave therapy for a model of liver cirrhosis ameliorates liver fibrosis and liver function. Sci Rep 2020;10:2405.
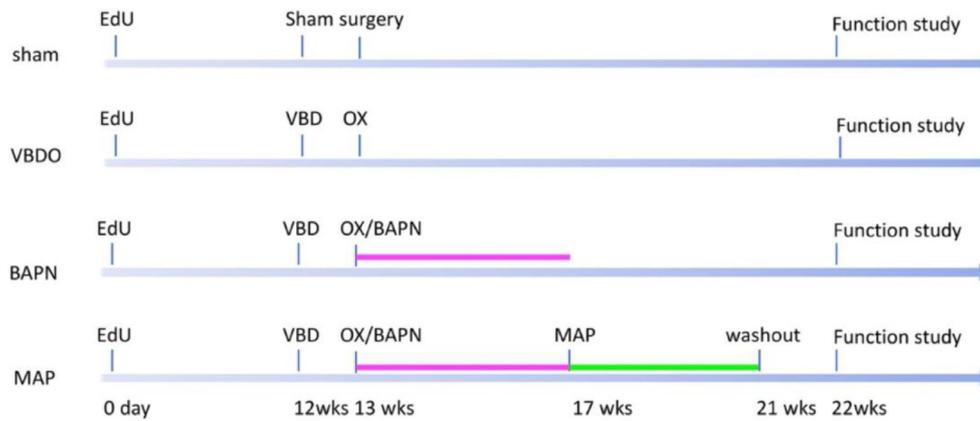
Figure S1 Experimental design of the MAP therapy experiment. Experimental protocol from day 0 to week 12. VBDO, vaginal balloon dilation and ovariectomy; BAPN, β-aminopropionitrile; MAP, microenergy acoustic pulse.
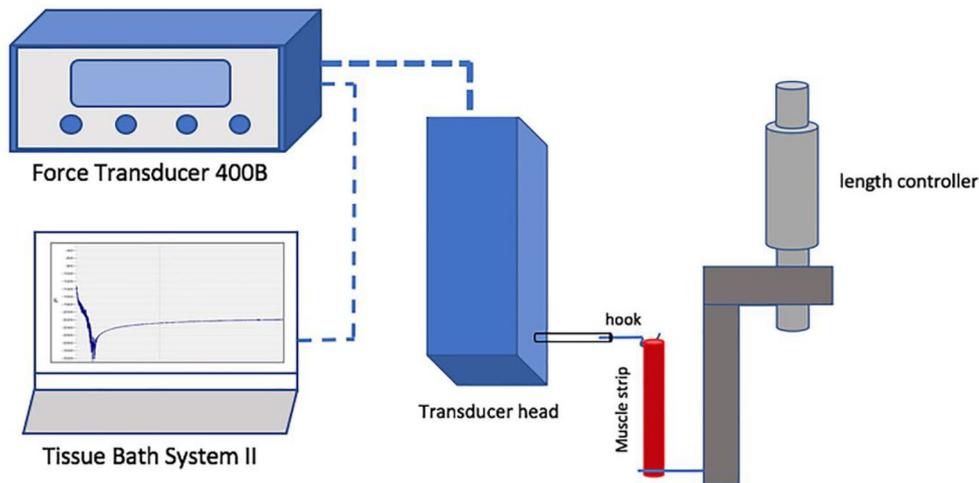

Figure S2 The muscular force transducer head and controller of 400B series of high-level output force transducers system. The muscular strip was hanged between the force sensor hook and force/length controller. Consistent 330-gram force was applied by the length controller, and the rebound force and muscular stiffness were recorded by the force sensor connected to a Myobath Tissue Bath System II.